Supporting Information

Permanent free radicals in bamboo biochar-based flow bed reactor: a sustainable solution for dye degradation via adsorption and radical oxidation

Paola Franchi,[a] Anna Turchetti,[a] Marco Lucarini,[a] Adolfo Manucci,[b] Marcello Pagliero,[b] Antonio Comite,[b] Alessandro Pellis,[b] Letizia Savio,[c] Elina Mkrtchian,[c] Giorgio Divitini,[d] Ambra Celotto,[d] Sergio Marras,[d] Tommaso del Rosso,[e] Sidnei Paciornik,[f], Silvana Alfei,[g] and Omar Ginoble Pandoli[d,g,h*]

[a] *Department of Chemistry "Giacomo Ciamician" Via P. Gobetti 85, 40129, Bologna, Italy.*
[b] *Department of Chemistry and Industrial Chemistry, University of Genoa, Via Dodecaneso, 31, 16148, Genoa, Italy.*
[c] *Istituto dei Materiali per l'Elettronica e il Magnetismo del Consiglio Nazionale delle Ricerche, UOS Genova, Via Dodecaneso 33, Genova, Italy.*
[d] *Istituto Italiano di Tecnologia (IIT), Via Morego 30, 16163, Genova, Italy.*
[e] *Departamento de Fisica, Pontifícia Universidade Católica, Rua Marque de São Vincente, 225, 22451-900, Rio de Janeiro, Brazil.*
[f] *Departamento de Engenharia Química e de Materiais, Pontifícia Universidade Católica, Rua Marque de São Vincente, 225, 22451-900, Rio de Janeiro, Brazil.*
[g] *Department of Pharmacy, University of Genoa, Viale Cembrano, 4, 16148 Genoa, Italy*
[h] *Departamento de Química, Pontifícia Universidade Católica, Rua Marquês de São Vincente, 225, 22451-900, Rio de Janeiro, Brazil.*
**Corresponding author: omar.ginoblepandoli@unige.it, omarpandoli@puc-rio.br, and omar.ginoble@iit.it*

Section S1. XRD Analyses

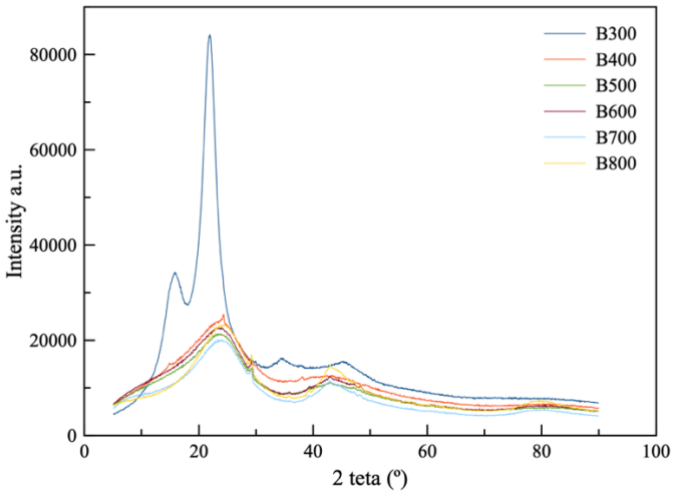

Figure S1. XRD analysis of BAC (B300-B800).

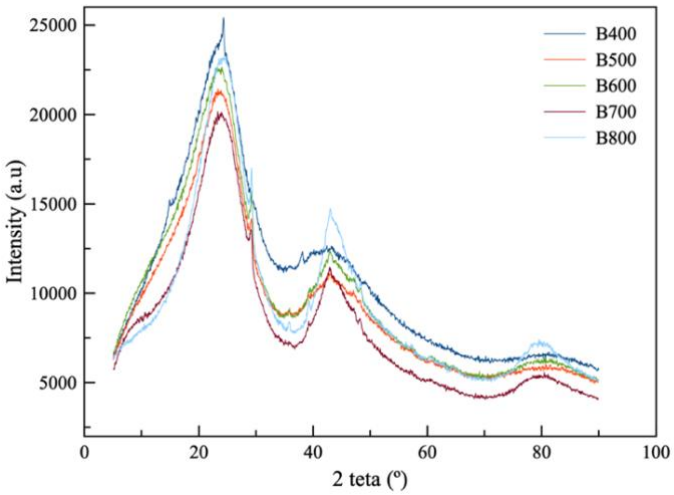

Figure S2. XRD analysis of BAC (B400-B800).

Section S2. SEM Analyses

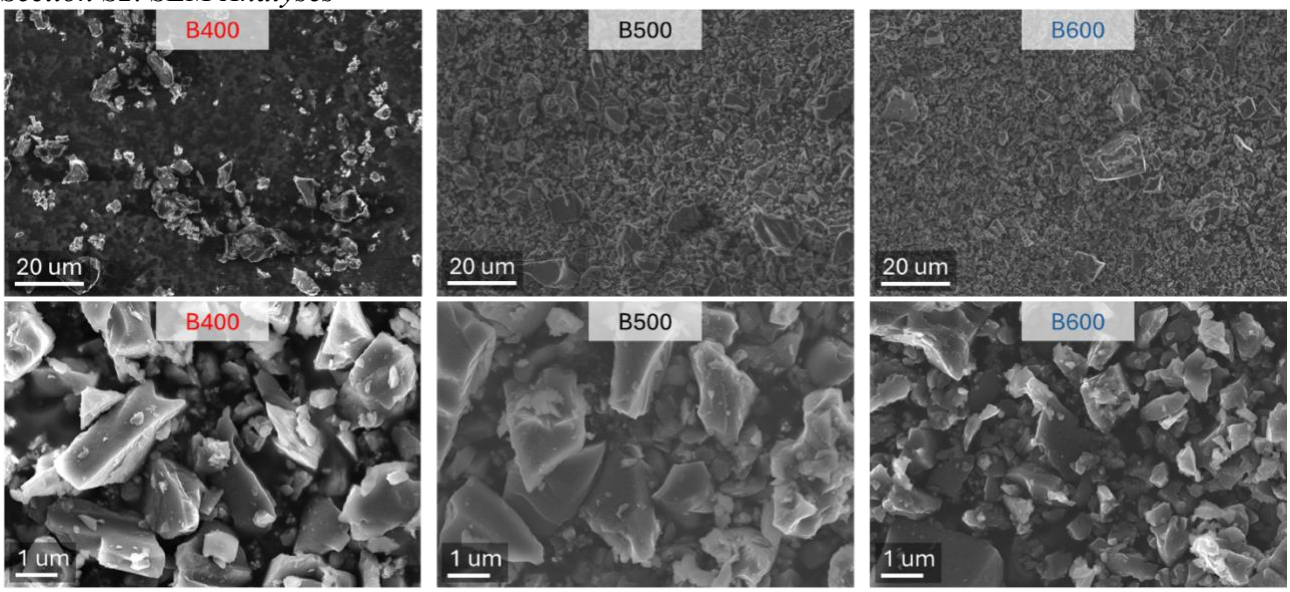

Figure S3. Scanning electron microscopy imaging of samples B400, B500 and B600. All samples present a broad size distribution and particles with sharp edges.

Section S3. Kinetic Studies

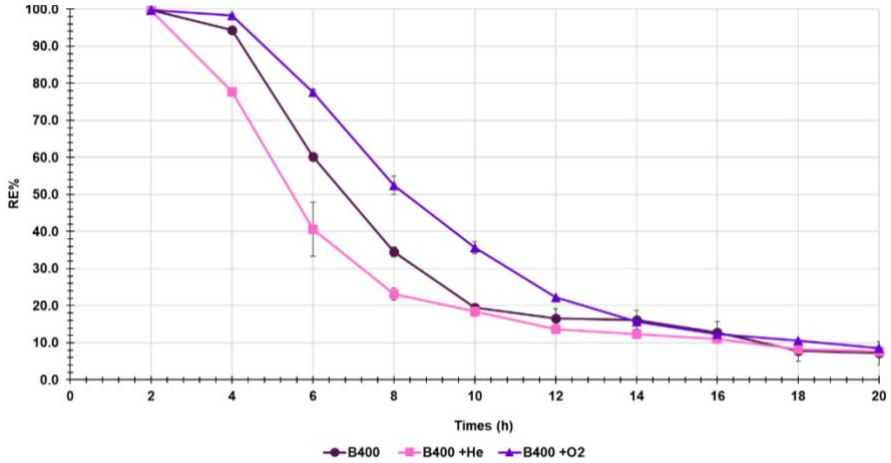

Figure S4. Loss of removal efficiency (RE%) over 20 hours-working in continuous flux of three column-packed removal systems (B400, B400 + insufflated He and B400 + insufflated O_2).

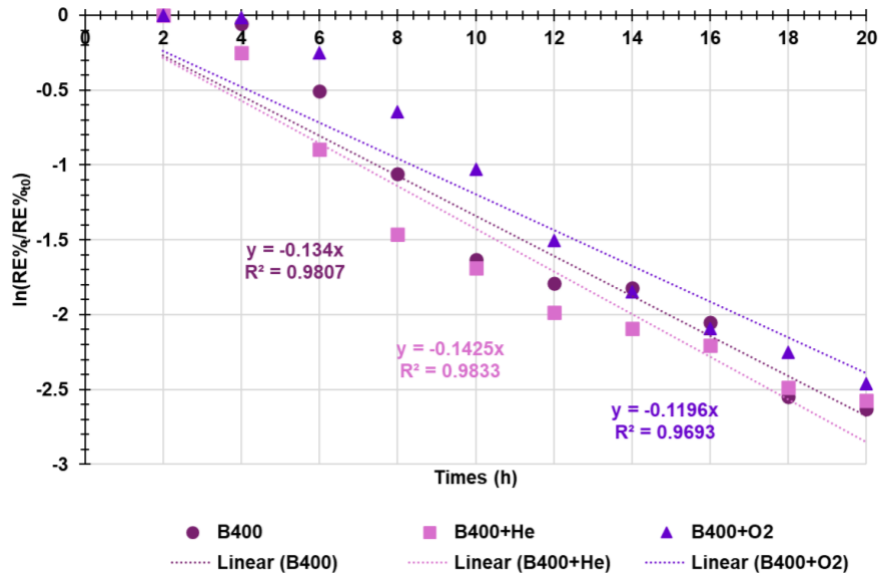

Figure S5. FO kinetic models.

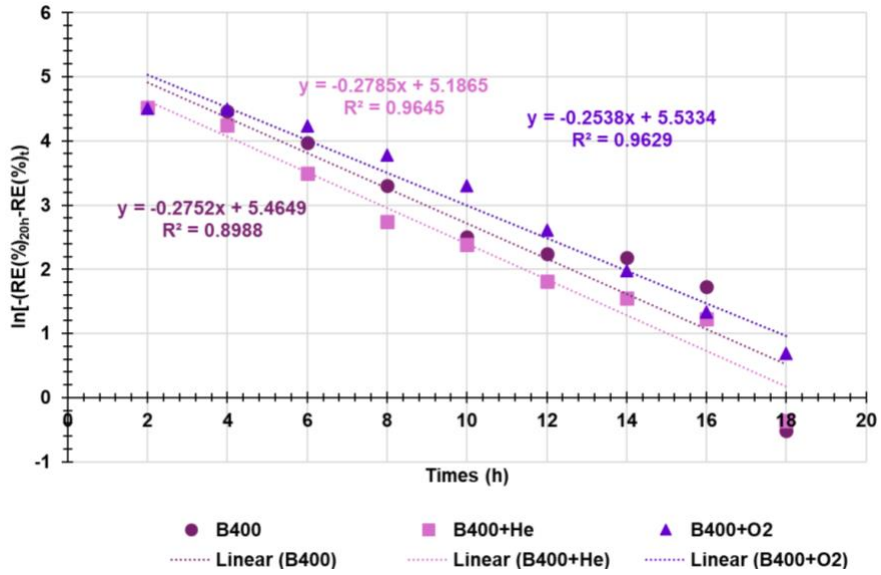

Figure S6. PFO kinetic models.

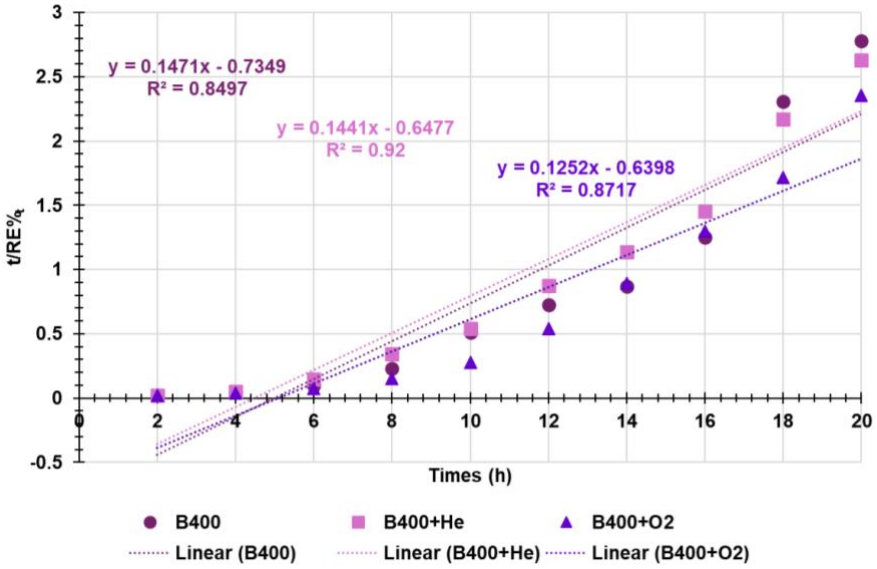

Figure S7. PSO kinetic models.

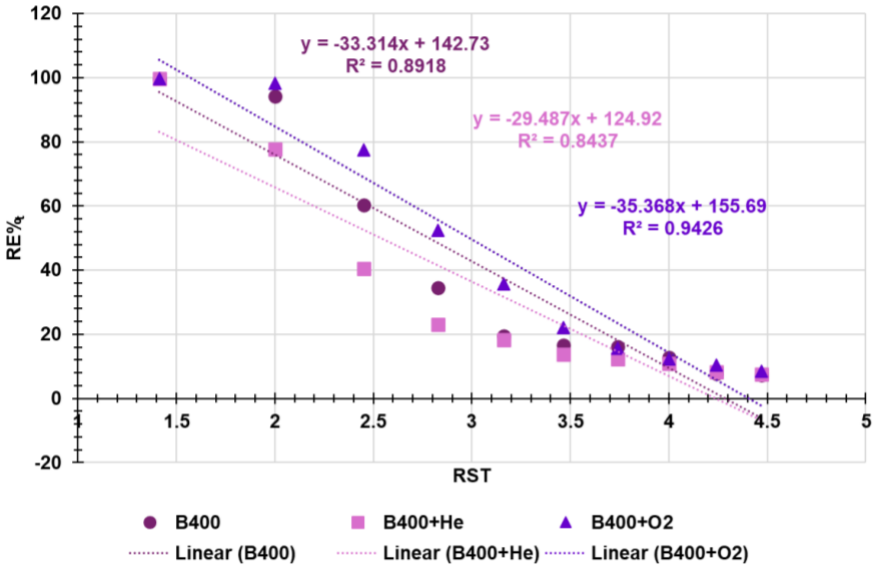

Figure S8. IPD kinetic models. RST = root square of times.

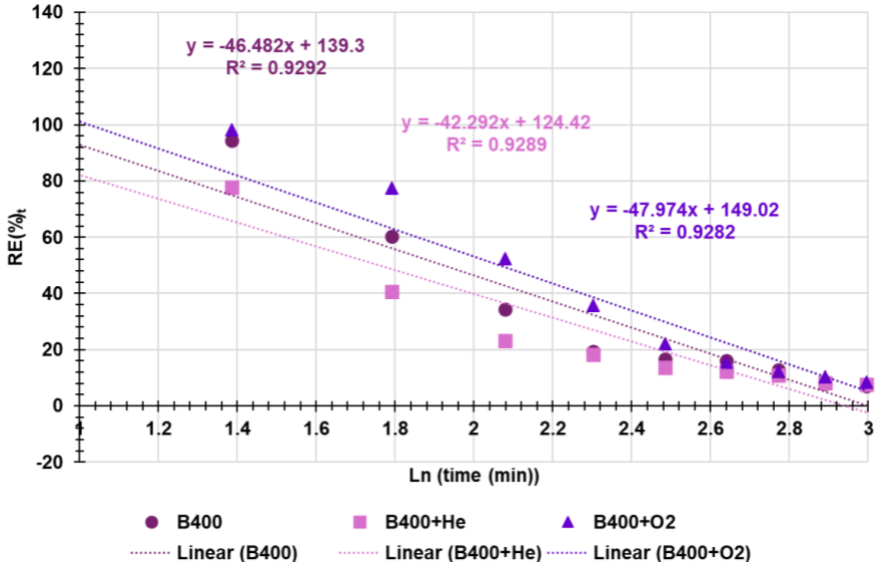

Figure S9. Elovich kinetic models.

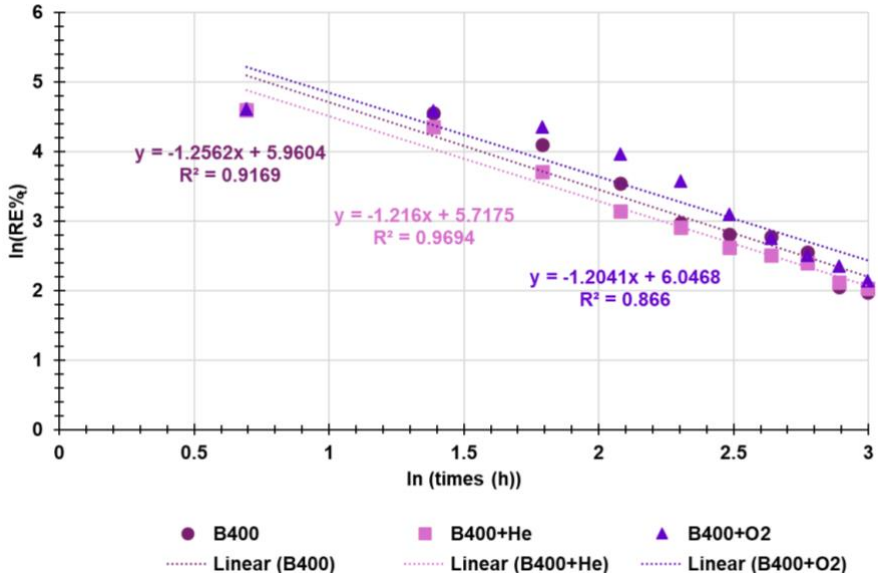

Figure S10. Korsmeyer Peppas kinetic models.

Table S1. R^2 values of all kinetic models considered for each removal system.

Models	R^2 B400	R^2 B400+He	R^2 B400+O_2
FO	**0.9807**	**0.9833**	**0.9693**
PFO	0.8988	**0.9645**	**0.9629**
PSO	0.8497	0.9200	0.8717
IPD	0.8918	0.8437	0.9426
ELO	0.9292	0.9289	0.9282
KMP	0.9169	**0.9694**	0.9327

PFO = Pseudo first order; PSO = pseudo second order; IPD = intra particle diffusion. ELO = Elovich; KMP = Korsmeyer Peppas. In bold the highest R^2 values > 0.95.

Table S2. Kinetic parameters for FO, PFO and Korsmeyer-Peppas models.

System	$RE\%_{20h\ EXP}$	$RE\%_{20h\ FO*}$	K_1	K_{PFO}	K_{KP}	n_{KP}

B400	7.2	3.4	0.308	0.6339	388	1.256
B400+He	7.6	2.9	0.328	0.6414	304	1.216
B400+O_2	8.5	3.6	0.275	0.5845	423	1.204

RE% = Removal efficiency percentage; EXP = experimental; PFO = pseudo-first order; KP = Korsmeyer Peppas. * The FO kinetic equation obtained without imposing the intercept equal to zero was used.

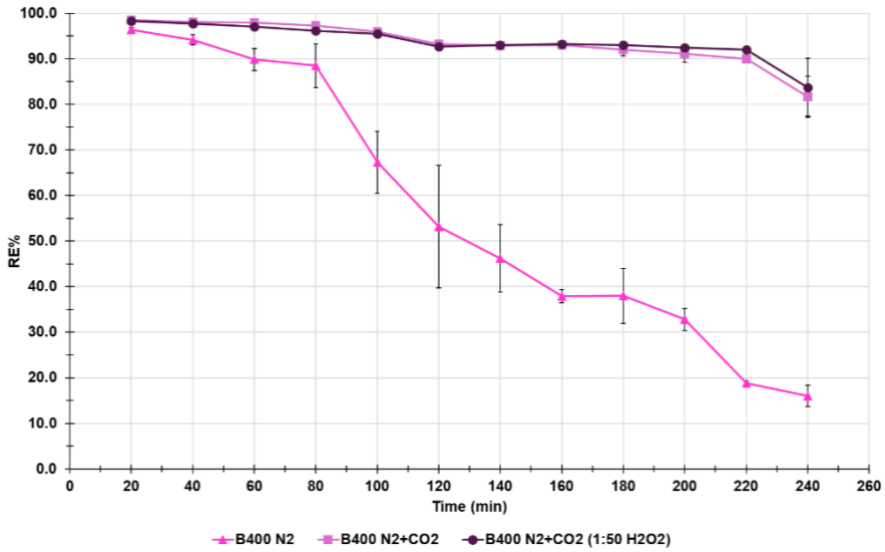

Figure S11. Graphical profiles of the removal efficiency loss (%) over time (240 min) of working in continuous flux of three columns filled with two different bamboo-based biochar obtained varying the pyrolysis conditions. One biochar was obtained by pyrolysis at 400°C under N_2 (fuchsia line with triangular markers), while the other was obtained by pyrolysis at 400°C under N_2 and CO_2 (pink and dark purple lines with squared and round markers, respectively). Columns were used to remove MB from MB solutions of concentration 2.5×10^-5 M (fuchsia and pink lines with triangular and squared markers). In one case added the MB solution was added with 1:50 H_2O_2 (dark purple line with round markers).

The data of removal efficiency loss (%) were modelled with the same kinetic models used in the previous section to reveal the main mechanisms that govern the rate of the processes. Figure S9-S14 show the dispersion graphs (indicators without lines) obtained for the six models and the related linear regression lines (dotted lines with the same colour of the indicators) with their equations and R^2 values. The linear regressions and their equations were provided by Microsoft Excel software 365 using the ordinary least square (OLS) method. The coefficients of determination (R^2) associated with all the equations have been reported in Table S3 and were considered as the parameters to determine which model best fits the RE% data according to the literature [1] as previously.

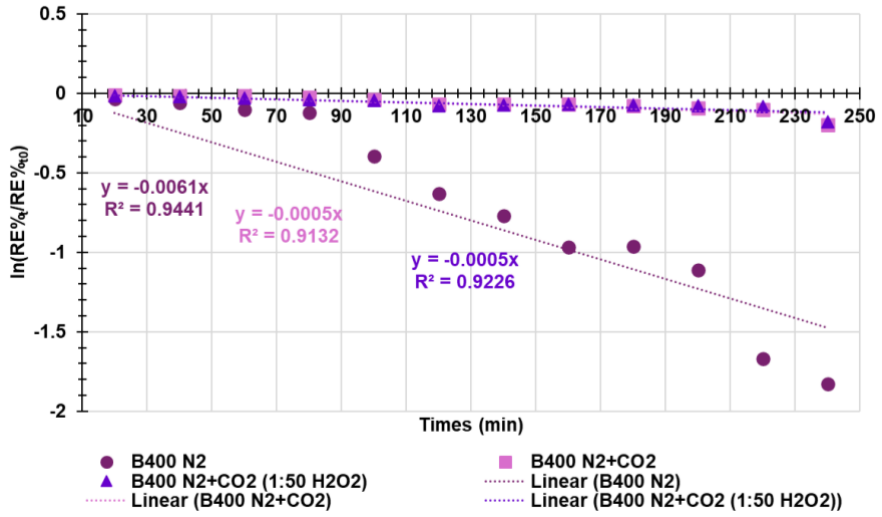

Figure S12. FO kinetic models.

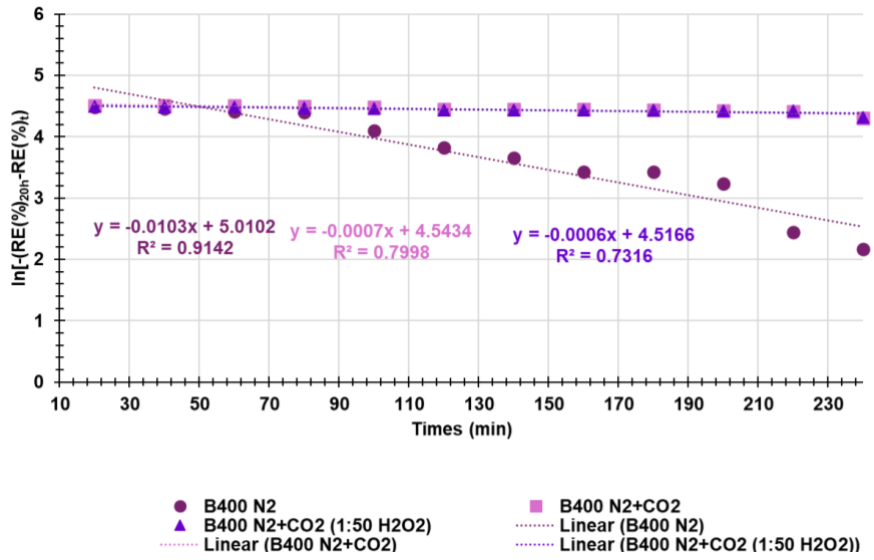

Figure S13. PFO kinetic models.

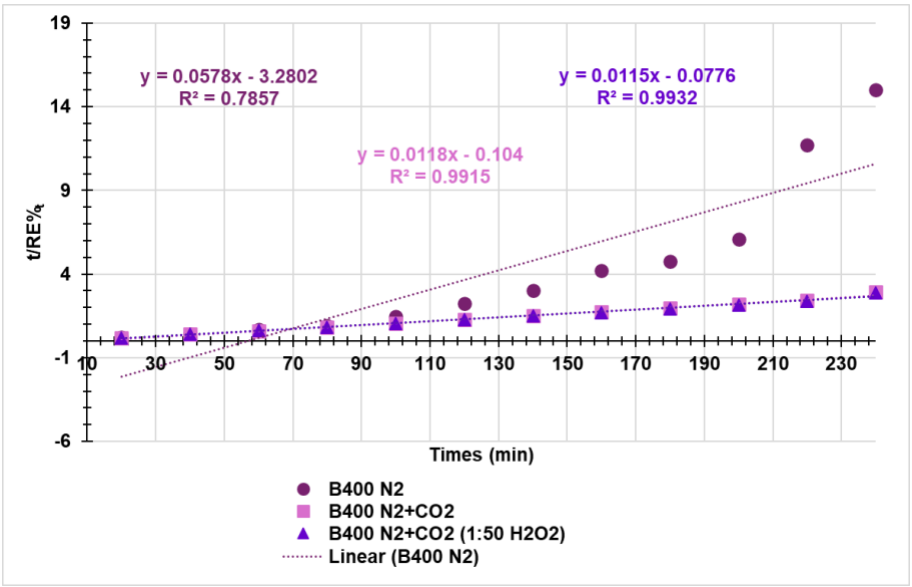

Figure S14. PSO kinetic models.

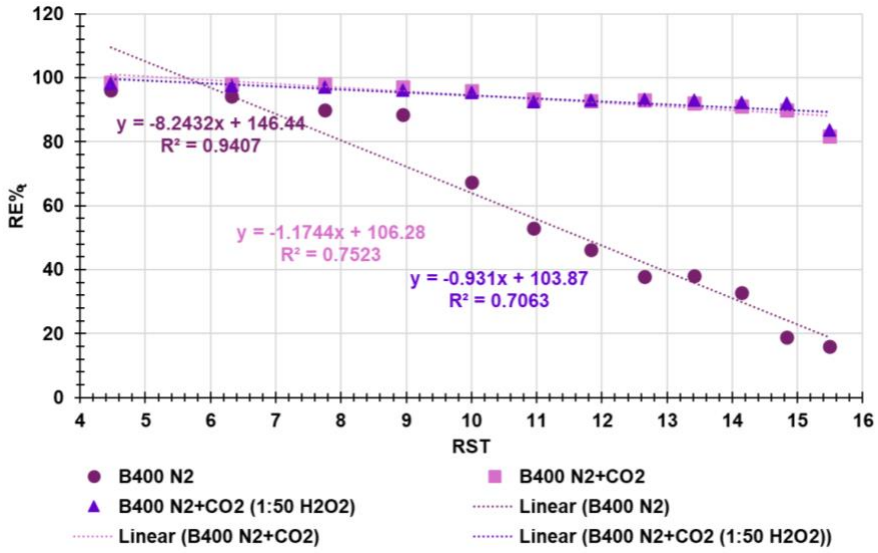

Figure S15. Intra particle diffusion kinetic models. RST = root square of times.

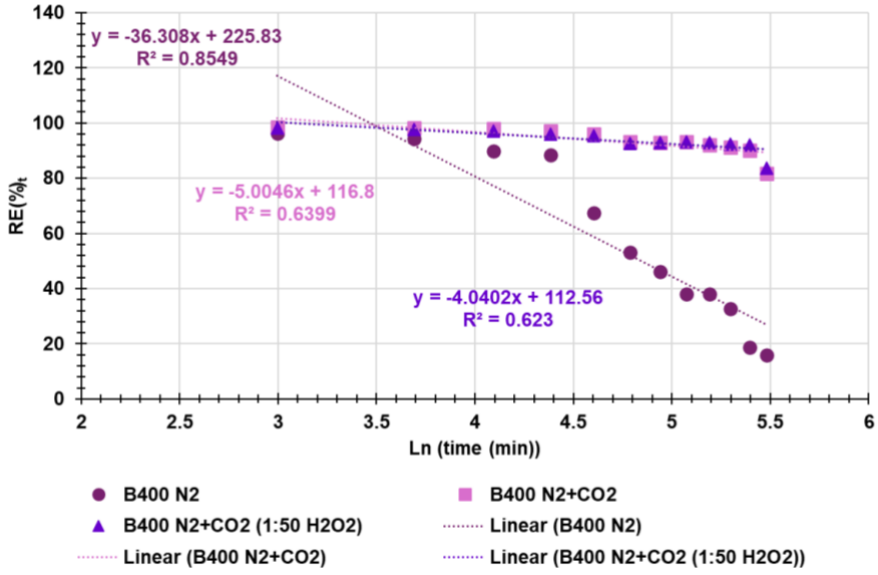

Figure S16. Elovich kinetic models.

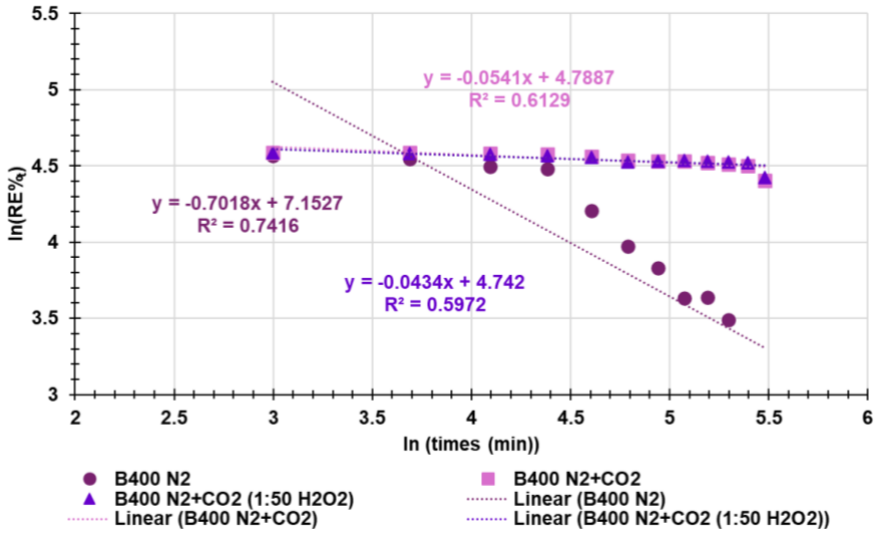

Figure S17. Korsmeyer Peppas kinetic models.

Table S3. R^2 values of all kinetic models considered for each column.

Models	R^2 B400 N_2	R^2 B400 N_2+ CO_2	R^2 B400 N_2+ CO_2+1:50 H_2O_2
FO	**0.9441**	0.9132	0.9226
PFO	0.9142	0.7998	0.7316
PSO	0.7875	**0.9915**	**0.9932**
IPD	**0.9407**	0.7523	0.7063
Elovich	0.8549	0.6399	0.6230
Korsmeyer-Peppas	0.7416	0.6129	0.5972

PFO = Pseudo first order; PSO = pseudo second order; IPD = intraparticle diffusion. In bold the highest R^2 values > 0.95.

The R^2 values obtained for the linear regression lines of all tested kinetic included in Table S3 evidenced that the loss of MB removal (%) efficiency over time (240 minutes of work in continuous flux) of the system made of the column filled with biochar obtained by pyrolysis at 400°C under only N_2 used to filtrate a MB solution without addition of H_2O_2 poorly fit all kinetic model ($R^2 < 0.95$) and the best fit was observed for FO and intra particle diffusion models ($R^2 = 0.9441$, and 0.9407). On the contrary, the removal systems made of the columns filled with biochar obtained by pyrolysis at 400°C under both N_2 and CO_2 used to filter MB solutions with and without addition of H_2O_2 almost perfectly fit the PSO kinetic model ($R^2 = 0.9915$ and 0.9932, respectively).

In the removal processes governed by the PSO kinetics, the velocity limiting step is considered chemical adsorption, including adsorption through the sharing or exchange of electrons between the adsorbent and the adsorbed, as in radical degradations, or electrostatic interactions [1–3]. On the other hand, compared to inert (N_2) atmosphere, CO_2, as a pyrolysis medium, promotes the biochar production yield within the temperature range between 400 and 600 °C for several biomasses [4]. Moreover, CO_2 is capable of significantly enhancing biochar features, such as surface area and porosity and can be used to modify other physiochemical properties such as elemental composition and chemical functional groups [4]. Additionally, larger specific surface area and rich porosities are conducive to stabilize PFRs in the biochar particles [5], thus enhancing biochar pollutants removal efficiency by oxidative degradation reactions and therefore slowing down its removal efficiency loss

(%) rate over time. In this regard, removal systems made of columns filled with biochar obtained under both N_2 and CO_2 atmosphere, in which PFRs are stabilized by higher surface area and porosity, are expected to remove MB by MB solutions mainly by oxidative degradation chemical reactions, due to the action of hydroxyl radicals formed by reaction of PFRs with O_2, H_2O and H_2O_2. On these considerations, the removal efficiency loss (%) in such systems was minimal (Figure 8), due to the degradative activity by reactive oxygen species (ROS) which supported for longer time the MB removal, thanks to the presence of stabilized PFRs. The fact that the removal efficiency loss experimental data of such systems almost perfectly fit the PSO kinetic model, confirmed that the albeit minimal removal efficiency loss (%) over time of these systems occurred mainly by the albeit minimal decay of PFRs acting as donors, acceptors, and/ or shuttles of electrons [1], which was limited by the PFRs higher stability. Interesting, there were no substantial differences in the removal efficiency loss (%) depending on the presence or absence of H_2O_2. On the contrary, with the removal system made of the column filled with biochar achieved under N_2 atmosphere, having not stabilized PFRs more susceptible to a faster decay, the removal efficiency loss over time was remarkably faster, being the contribute of the oxidative degradation chemical reactions to MB removal limited over time. The fact that the removal efficiency loss (%) experimental data do not fit PSO kinetics confirmed that chemical reactions were scarcely involved in the MB removal.

Table S4 contains important kinetic parameters of FO, PSO and intraparticle diffusion (IPD) models calculated according to literature from the equations reported in the Figure S12, S14 and S15 [1–3].

Table S4. Kinetic parameters for FO, PSO and IPD.

System	$RE\%_{240min\ EXP}$	$RE\%_{240min\ PSO}$	K_1	K_{PSO}	K_{IPD}
B400 N_2	16.0	17.3	0.0140	90.9	8.2432
B400 N_2+CO_2	81.7	84.7	0.0011	68972.0	1.1744
B400 N_2+CO_2 1:50 H_2O_2	83.7	87.0	0.0011	99327.8	0.9310

EXP = Experimental; RE = removal efficiency; PSO = pseudo-second order; K_1 = rate constant of FO kinetic model; K_{IPD} = rate constant of IPD kinetic model; K_{PSO} = rate constant of PSO kinetic model (since K PSO is at the denominator in PSO equation, unlike in other cases, higher values of K mean a lower rate of removal efficiency loss (%).

The rate constants of all kinetic models were calculated for all removal systems and conditions although the experimental data scarcely fit them, while the RE% at the max time considered of 240 minutes ($RE\%_{240min}$) was calculated using the equation of PSO kinetic model. All rate constants confirmed that the removal efficiency loss (%) of systems using biochar prepared in CO_2 atmosphere was minimal and remarkably slower than that of system using biochar prepared only in N_2 atmosphere having less stabilized PRFs. On the contrary, no substantial differences were observed in presence or

not of 1:50 H_2O_2. The RE% values after 240 hours of treatment predicted by the PSO model well agreed with the experimental ones, especially for systems using biochar prepared in CO_2 atmosphere which best fit this model (errors of +3.5 and +3.7%), respect to the system prepared in N_2 atmosphere (error of -5.9%), due to its poor fitting with this model. Anyway, the good agreement established that the diffusion stage within the particle was scarcely involved in the mechanism of the removal process and in those governing the removal efficiency loss [2,6].

References

[1] F. Zanardi, F. Romei, M.N.B. Junior, S. Paciornik, P. Franchi, M. Lucarini, A. Turchetti, L. Poletti, S. Alfei, O.G. Pandoli, Pivotal Contribute of EPR-Characterized Persistent Free Radicals in the Methylene Blue Removal by a Bamboo-Based Biochar-Packed Column Flow System, ChemCatChem 16 (2024). https://doi.org/10.1002/cctc.202401042.

[2] S. Alfei, V. Orlandi, F. Grasso, R. Boggia, G. Zuccari, Cationic Polystyrene-Based Hydrogels: Low-Cost and Regenerable Adsorbents to Electrostatically Remove Nitrites from Water, Toxics 11 (2023) 312. https://doi.org/10.3390/toxics11040312.

[3] S. Alfei, F. Grasso, V. Orlandi, E. Russo, R. Boggia, G. Zuccari, Cationic Polystyrene-Based Hydrogels as Efficient Adsorbents to Remove Methyl Orange and Fluorescein Dye Pollutants from Industrial Wastewater, Int J Mol Sci 24 (2023) 2948. https://doi.org/10.3390/ijms24032948.

[4] P. Premchand, F. Demichelis, D. Chiaramonti, S. Bensaid, D. Fino, Biochar production from slow pyrolysis of biomass under CO2 atmosphere: A review on the effect of CO2 medium on biochar production, characterisation, and environmental applications, J Environ Chem Eng 11 (2023) 110009. https://doi.org/10.1016/j.jece.2023.110009.

[5] X. Liu, Z. Chen, S. Lu, X. Shi, F. Qu, D. Cheng, W. Wei, H.K. Shon, B.-J. Ni, Persistent free radicals on biochar for its catalytic capability: A review, Water Res 250 (2024) 120999. https://doi.org/10.1016/j.watres.2023.120999.

[6] H. Khatooni, S.J. Peighambardoust, R. Foroutan, R. Mohammadi, B. Ramavandi, Adsorption of methylene blue using sodium carboxymethyl cellulose-g-poly (acrylamide-co-methacrylic acid)/Cloisite 30B nanocomposite hydrogel, J Polym Environ 31 (2023) 297–311. https://doi.org/10.1007/s10924-022-02623-x.